*Int. J. Electrochem. Sci.*, 16 **(2021)** Article ID: 210911, doi: 10.20964/2021.09.11

International Journal of
ELECTROCHEMICAL
SCIENCE
www.electrochemsci.org

*Short Communication*

# Monitoring of Monocrystalline Silicon PERC Solar Cell with Laser-Doped Selective Emitter Using Infrared and Electroluminescence Imaging

*Zhan Wang, Fuyang Chen*[*]

School of Automation Engineering, Nanjing University of Aeronautics and Astronautics, Nanjing, 211106, China
[*]E-mail: fuyang_chen001@163.com

*Received:* 2 May 2021/ *Accepted:* 21 June 2021 / *Published:* 10 August 2021

In this study, a new selective emitter (SE) technology was used in the mass production line for monocrystalline silicon PERC cells. The internal quantum efficiency and series resistance scanning of the SE cells in the early stage of upgrading was examined from the standpoint of test and control, to offer guidance for the most efficient scheme of the new SE technology. The quality risk assessment of the performance of the newly upgraded SE and conventional PERC modules were carried out using infrared thermal imaging, electroluminescence, and other test and control methods, which provides technical support for the automatic detection of defects such as electroluminescence of modules and infrared thermal imaging of power stations. The test results show that if the newly upgraded SE-PERC and conventional PERC cells were mixed to make modules in mass production of PERC line, the electroluminescence uneven light and shade phenomenon will appear in the modules, and were more obvious after light attenuation. The phenomenon of uneven light and dark was caused by the difference of open-circuit voltage or conversion efficiency between the two cells. Through the IR test, the surface temperature of the darkened cell was about 20 °C higher than that of the brightened cell, which will bring a greater risk of a hot spot in the actual use of the module. At the same time, in the process of using the power station, the defective modules were identified by infrared thermal imaging detection, and the defective modules were replaced in time to ensure the normal power generation of the photovoltaic power station.

**Keywords:** Selective emitter; Passivated emitter and rear contact; Infrared thermal imaging; Electroluminescence; Automatic detection

## 1. INTRODUCTION

With the introduction of the leader, new technologies such as passivated emitter and rear contact (PERC), double-sided, N-type, half chip, multiple bus bar (MBB), metallization wrap through (MWT), black silicon, and so on have been developed rapidly [1-3]. Among them, PERC has become

a necessary technology widely used. To achieve full score modules, it is necessary to integrate other technologies on PERC technology [4, 5].

Selective emitter (SE) technology has been paid attention by first-line enterprises because of its low cost and significant efficiency improvement [6, 7]. At present, a certain scale of SE technology has been used in the production of battery chips by first-line module enterprises such as Jinko, Longi, JA, Trina, Aiko, etc [8, 9]. The combination of "SE-PERC" can easily meet the requirements of full score modules. At present, only Aiko Solar, which has the largest capacity, has an annual capacity of 5GW [10, 11]. SE technology is expected to become a new technology widely used in the industry after PERC [12, 13].

In this study, the actual situation of SE technology in the mass production of monocrystalline silicon PERC production line upgrade was aimed, and the SE-PERC cell was tested and analyzed by Internal Quantum Efficiency (IQE), Core Scan, and other testing means provide direction for the optimal scheme of the PERC cell in the production line to obtain the highest efficiency. Due to the new technology online, in the early stage of the process switching, two kinds of battery chips, SE-PERC and conventional PERC will appear in the production line at the same time [14, 15]. The two kinds of battery chips cannot be distinguished in appearance, and can only be distinguished in the process sheet. Because at the electrical performance test end of the battery chip, if the two kinds of batteries are to be tested separately, it will have a great impact on manpower and production cost [16, 17]. Considering the above problems, the two kinds of cells on the production line may be tested together, so there will be the phenomenon of mixed operation of the two kinds of cells at the module end. In this study, the performance of new and old cell mixed technologies was examined using infrared and electroluminescence imaging to check if there was a quality risk at the module end using the design of experiments.

## 2. MATERIALS AND METHOD

### *2.1 Preparation of SE-PERC cells*

The preparation of the cell chip was carried out on the mass production line of monocrystalline silicon PERC cell and the laser phosphorus silicate glass (PSG)doping method was adopted in the SE process. The heavily doped region was formed by laser scanning using the phosphor silicon glass layer generated by diffusion as the doping source [1]. P-type mono-crystalline Si wafers with 170μm thick and 5-inch diameter were used. Conventional furnace diffusion formed a low-doped emitter together with a PSG. A pulsed neodymium-doped yttrium aluminum garnet laser with a wavelength of 532nm, pulse frequency of 20 kHz, and laser beam size of 5μmx250μm was used to scan the wafer surface. The irradiation of laser locally melted the silicon and extra phosphorus atoms diffused from the PSG layer in the melt. After laser irradiation, the standard industrial process was proceeding. The PSG layer was acted as a doping precursor. Then, hydrofluoric acid removed the PSG layer and a coating of SiNx anti-reflection was deposited using plasma-enhanced chemical vapor deposition. Finally, screen firing and printing of the back and front contacts completed the solar cell. The SE and conventional PERC

cells with the same efficiency were tested and analyzed by Internal Quantum Efficiency and Core Scan, respectively.

*2.2 Preparation of mixed cell module for SE-PERC and conventional PERC*

In the process of selecting a cell chip, three experimental schemes were adopted: group A adopted SE and conventional PERC monocrystalline silicon cells with the same efficiency gear; group B adopted SE and conventional monocrystalline silicon PERC cells with the same opening voltage; group C adopted SE and conventional monocrystalline silicon PERC cells with low efficiency gear and mainstream gear. Under the same assembly process conditions, two kinds of cells in each group were combined and packaged into 60 or 70 pieces of assembly by using the same packaging materials and process. After packaging, the experimental modules were tested by electroluminescence and IV (under STC condition). Then, the module was put into the steady-state box, with the irradiance of 1000±50W/m$^2$, the temperature of 60±5$^o$C, and after 5h light attenuation, the infrared thermal imager was used to photograph the surface temperature of the cell, and observe the temperature difference of the cell at different positions; and after 4 days of outdoor exposure, the electroluminescence and IV test was carried out again to investigate the attenuation and the brightness of the cell.

## 3. RESULTS AND DISCUSSION

*3.1 Electrical performance test of battery*

After upgrading SE-PERC technology for the first time in a conventional PERC production line, the relative values of the electrical performance of SE-PERC cells and conventional PERC cells are summarized in table 1.

**Table 1.** Comparison of electrical performance between SE and conventional PERC cells

| Cells | $U_{OC}$ (mV) | Jsc (mA/cm$^2$) | FF (%) | $E_{ta}$ (%) |
|---|---|---|---|---|
| **Conventional-PERC** | 583 | 28.9 | 76.2 | 12.8 |
| **SE-PERC** | 596 | 32.6 | 72.8 | 14.2 |
| **△** | 13 | 3.7 | -3.4 | 1.4 |

As shown in Table 1, the Solar cell efficiency (ETA) of SE-PERC increased (ETA=14.2%) compared to conventional PERC (ETA = 12.8%). The enhanced efficiency can be attributed to the less recombination in the lower-doped emitter and better surface passivation by the SiNx layer. Thus, the short-circuit current density ($J_{sc}$) and open-circuit voltage ($U_{oc}$) increase by ΔJsc=3.7 mA/cm$^2$ and ΔUoc=13 mV. The lower doping between the contact fingers leads to a higher series resistance which decreases the fill factor by ΔFF = 3.4% compared to the conventional PERC cells.

*3.2 Internal Quantum Efficiency test of cell chip*

Three SE cells and three conventional PERC cells with the same efficiency were selected. By PL test, the representative area of each cell was selected as the test object. To eliminate the influence of reflectivity on quantum efficiency, the reflectivity of each cell was tested firstly, and then the quantum efficiency in the range of 300-1100nm was tested to get the IQE curve.

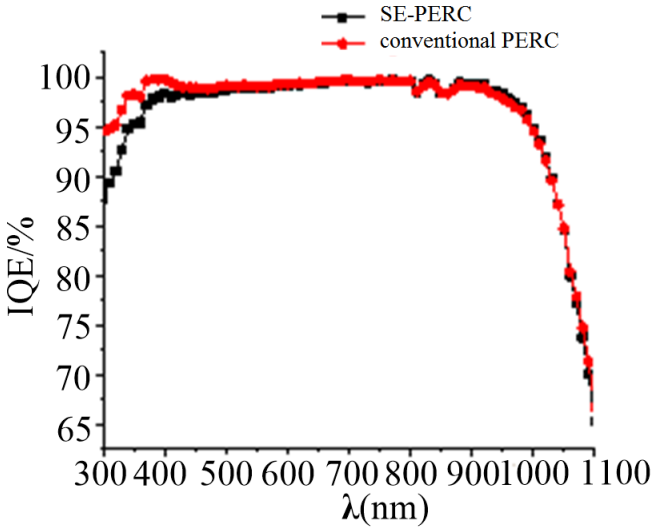


**Figure 1.** Internal Quantum Efficiency of SE and conventional PERC cells

As shown in figure 1, the IQE of SE-PERC cell in the 350-800nm band was higher than that of conventional PERC cell. In the 350-500nm band, it reflects the absorption of light by the diffusion layer, because the SE cell adopts the process of light doping between the thin gate lines and the heavy doping of the thin gate lines. The shallow diffusion layer can improve the quantum efficiency of the solar light in the short band 350-500nm, increase the short circuit current and open-circuit voltage, to improve the efficiency [18]. In 500-800nm band, it reflects the characteristics of the PN junction layer [19]. There is a horizontal ($n^{++}$-$n^{+}$) high and low junction in SE-PERC cell, which can improve $U_{OC}$ and efficiency. Therefore, when the production line of conventional PERC cell appears SE technology upgrade, to give full play to the advantages of SE cell, and to optimize the efficiency of SE-PERC cell, the process should consider how to improve its IQE in 350-500nm and 500-800nm band [20, 21]. From the IQE curve in Figure 1, the IQE of the newly upgraded SE-PERC cell was not significantly improved in the 500-800nm band, so it was necessary to further improve the quantum efficiency of the SE-PERC cell in the 500-800nm band.

*3.2 Core Scan test of cell chip*

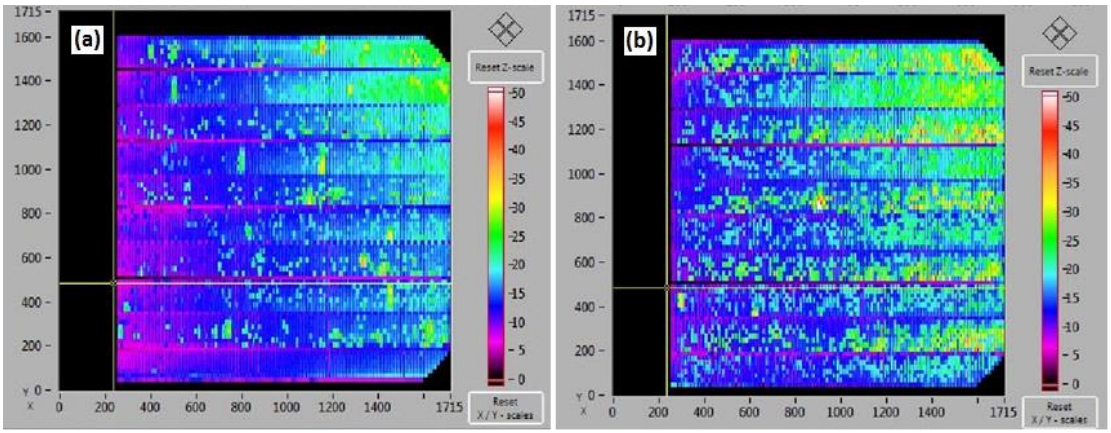


**Figure 2.** (a) Conventional PERC and (b) SE-PERC Core Scan at scan line spacing 1.5 min and scan speed 20 mm/s

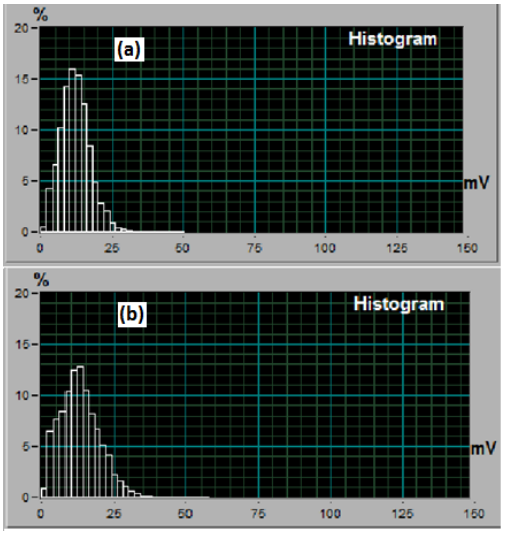


**Figure 3.** Potential distribution of (a) conventional PERC and (b) SE-PERC

**Table 2.** Potential of SE and conventional PERC cells

| Cells | Maximum Potential/mV | Average Potential/mV | Percentage greater than 15 mV |
|---|---|---|---|
| SE-PERC | 56.6 | 13.2 | 74.05% |
| Conventional PERC | 48.3 | 12.0 | 64.65% |

**Table 3.** Sheet resistance and contact resistance

| Cells | Contact resistance $R_c$/mΩ | Sheet resistance $R_{sheet}$/mΩ |
|---|---|---|
| SE-PERC | 3.4 | 4.9 |
| Conventional PERC | 2.9 | 3.9 |

Because the square resistance of the SE-PERC cell is quite different from that of a conventional PERC cell, it will lead to the difference of Rs and FF between the two kinds of cells. Therefore, the Core Scan function of the Core Scan device was used to test and analyze the Rs of cells [22]. Figure 2 indicates the Core Scan of conventional PERC and SE-PERC. Figure 3 indicates the potential distribution of conventional PERC and SE-PERC. The average value and distribution of the potential of the following cells and the comparative analysis of the thin layer resistance and contact resistance were obtained respectively. The results are summarized in Tables 2 and 3.

As shown, the average potential of the newly upgraded SE-PERC cell was higher than that of the conventional PERC cell. The thin layer resistance and contact resistance of SE-PERC cell was higher than those of conventional PERC cell, so the FF of SE-PERC cell was lower than that of conventional PERC cell [23, 24]. The thin layer resistance of the SE-PERC cells was high because of the high square resistance in the light doping region, which leads to the low FF. In addition, the contact resistance of SE-PERC cells in the heavily doped regions is too large, which indicates that the doping concentration is low, so it is necessary to further increase the doping concentration, to reduce the contact resistance and improve the FF. Therefore, to improve the FF of SE-PERC cell and further improve the efficiency of SE-PERC cell, it is necessary to consider the matching of the square resistance of lightly doped region and heavily doped region [25, 26].

### *3.3 Test of mixed module of SE and conventional PERC cell*

Combined with the actual situation of the new technology upgrade of the production line, to evaluate the reliability risk of the new and old batteries mixed into modules, the modules of the three schemes are tested by light attenuation, electroluminescence, and IR respectively. The results are shown in figures 4 and 5.

**Table 4.** Electrical performance degradation percentage of different modules after 5 hours exposure in the light attenuation box

| Group | $I_{sc}$[a] | $U_{oc}$[b] | $I_{mpp}$[c] | $U_{mpp}$[d] | $P_{mpp}$[e] | FF[f] |
|---|---|---|---|---|---|---|
| A | 0.71% | 0.08% | 0.59% | 0.45% | 1.04% | 0.25% |
| B | 1.08% | 0.22% | 1.24% | 0.59% | 1.82% | 0.53% |
| C | 0.80% | 0.38% | 0.93% | 0.97% | 1.89% | 0.72% |

[a]Short-circuit current; [b]Open-circuit voltage; [c]Maximum Power Point Current; [d]Maximum power point voltage; [f]Fill factor

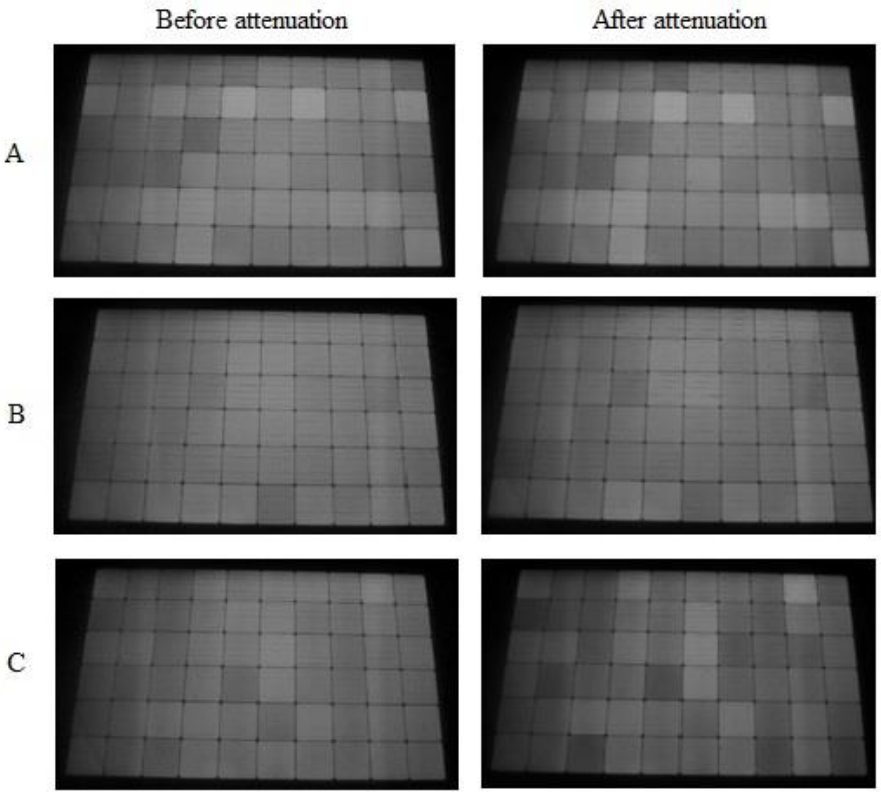


**Figure 4.** Comparison of electroluminescence images before and after 5 hours exposure in the light attenuation box

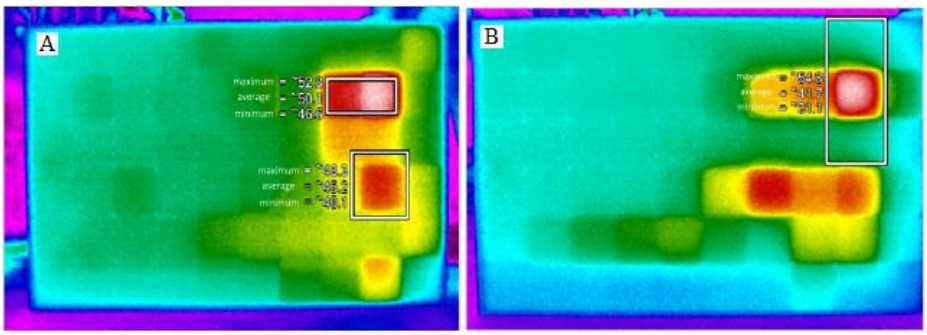


**Figure 5.** Comparison of IR images of light attenuation box after 4 days exposure to sunlight (a) Blackened cell and (b) Brighter cell

According to the light attenuation data in Table 4, the modules made of three different mixed-modes of the cell all show different degrees of power attenuation after 5 h exposure in the light attenuation box. According to the electroluminescence image in Figure 4, the electroluminescence of group A's mixed mode modules before and after the light attenuation shows obvious uneven brightness

of the cell. The electroluminescence of SE-PERC cell with the same efficiency gear was bright, while the electroluminescence of conventional PERC cell with the same efficiency gear was dark [27, 28]. Because the open-circuit voltage of SE-PERC cell with the same efficiency gear was higher than that of conventional PERC [29, 30]. In group B, with the same switching voltage, the electroluminescence brightness of the modules made of SE and conventional PERC cells was not obvious before light attenuation, but it was not increased after light attenuation. Under the same opening voltage, the efficiency of SE-PERC was low, while that of conventional PERC was high, so the darkening phenomenon was obvious after light attenuation, and the light attenuation power of group B was the largest [31, 32]. In group C, low-efficiency gear SE cell and monocrystalline silicon PERC cell with mainstream gear common were mixed into the module. After light attenuation, the phenomenon of electroluminescence unevenness was obvious [33]. The electroluminescence of SE cells in low-efficiency gear was dark, and the attenuation was greater [34, 35]. Combined with the IR test results in Figure 5, the surface temperature of the blackened cell in the electroluminescence image is higher than 50 $^{o}$C by using the infrared thermal imager, while the surface temperature of the brighter cell in the electroluminescence image was lower, only about 30 $^{o}$C. In contrast, this kind of dark cell was more likely to have hot spots in the actual use process of later modules.

From the perspective of automatic online detection control, the modules that can be detected and identified by the light and dark image visual method of module electroluminescence can be detected and filtered by 100% online detection to ensure the quality of product delivery [36].

## 4. CONCLUSIONS

Three different mixed modes of SE-PERC and conventional PERC are designed through experiments. The test results show that if the newly upgraded SE-PERC and conventional PERC cells were mixed to make modules in mass production of PERC line, the electroluminescence uneven light and shade phenomenon will appear in the modules, and were more obvious after light attenuation. The phenomenon of uneven light and dark was caused by the difference in open-circuit voltage or conversion efficiency between the two cells. Through the IR test, the surface temperature of the darkened cell was about 20 $^{o}$C higher than that of the brightened cell, which will bring a greater risk of a hot spot in the actual use of the module. At the same time, in the process of using the power station, the defective modules were identified by infrared thermal imaging detection, and the defective modules were replaced in time to ensure the normal power generation of the photovoltaic power station.

## References

1. A. Longacre, M. Martin, T. Moran, O.V. Kolosov, E. Schneller, A.J. Curran, M. Wang, J. Dai, L.S. Bruckman and J.-N. Jaubert, *Journal of Materials Science*, 55(2020)11501.
2. J. Walter, L.C. Rendler, C. Ebert, A. Kraft and U. Eitner, *Energy Procedia*, 124(2017)515.

3. Z. Zhang, C. Luo and Z. Zhao, *Natural Hazards*, 104(2020)2511.
4. X. Jia, C. Zhou, Y. Tang and W. Wang, *Solar Energy Materials and Solar Cells*, 227(2021)111112.
5. Z. Zhang, M. Liu, M. Zhou and J. Chen, *International Journal of Approximate Reasoning*, 126(2020)84.
6. W. Wu, Z. Zhang, F. Zheng, W. Lin, Z. Liang and H. Shen, *Progress in Photovoltaics: Research and Applications*, 26(2018)752.
7. X. Liu, R. Rao, J. Shi, J. He, Y. Zhao, J. Liu and H. Du, *Journal of Alloys and Compounds*, 875(2021)159999.
8. T. Dullweber, M. Stöhr, C. Kruse, F. Haase, M. Rudolph, B. Beier, P. Jäger, V. Mertens, R. Peibst and R. Brendel, *Solar Energy Materials and Solar Cells*, 212(2020)110586.
9. Z. Dai, J. Xie, X. Fan, X. Ding, W. Liu, S. Zhou and X. Ren, *Chemical Engineering Journal*, 397(2020)125520.
10. Y. Zhang, G. Liu, C. Zhang, Q. Chi, T. Zhang, Y. Feng, K. Zhu, Y. Zhang, Q. Chen and D. Cao, *Chemical Engineering Journal*, 392(2020)123652.
11. L. Mo, L. Zhao, C. Zhou, G. Wang, X. Jia and W. Wang, *International Journal of Electrochemical Science*, 15(2020)11920.
12. Z. Hou, H. Lu, Y. Li, L. Yang and Y. Gao, *Frontiers in Materials*, 8(2021)91.
13. Z. Zhang, X. Liu, Y. Zhang, M. Zhou and J. Chen, *Mechanical Systems and Signal Processing*, 135(2020)106389.
14. T.-C. Chen, S. Yu and Z.-P. Yang, *Applied Surface Science*, 521(2020)146386.
15. Z. Yao, L. Zhao, H. Diao and W. Wang, *Int. J. Electrochem. Sci*, 15(2020)8220.
16. S. Joonwichien, Y. Kida, M. Moriya, S. Utsunomiya, K. Shirasawa and H. Takato, *Solar Energy Materials and Solar Cells*, 186(2018)84.
17. M. Liu, Z. Xue, H. Zhang and Y. Li, *Electrochemistry Communications*, 125(2021)106974.
18. L. Tang, L.M. Fraas, Z. Liu, Y. Zhang, H. Duan and C. Xu, *Solar Energy Materials and Solar Cells*, 194(2019)137.
19. M.J. Mendes, S. Morawiec, I. Crupi, F. Simone and F. Priolo, *Energy Procedia*, 44(2014)184.
20. Z. Li, Y. Zhao, X. Wang, Y. Sun, Z. Zhao, Y. Li, H. Zhou and Q. Chen, *Joule*, 2(2018)1559.
21. M. Sun, B. Hou, S. Wang, Q. Zhao, L. Zhang, L. Song and H. Zhang, *Environmental Science: Water Research & Technology*, 7(2021)396.
22. A. Fiory, *Journal of electronic materials*, 31(2002)981.
23. A.S.D. Martha and H.B. Santoso, *Journal of educators Online*, 16(2019)1.
24. Z. Chen, H. Zhang, X. He, G. Fan, X. Li, Z. He, G. Wang and L. Zhang, *BioResources*, 16(2021)2644.
25. C. Zhang, H. Shen, L. Sun, J. Yang, S. Wu and Z. Lu, *Energies*, 13(2020)1388.
26. L. Zhang, H. Wang, X. Zhang and Y. Tang, *Advanced Functional Materials*, 31(2021)2010958.
27. Y.-N. Chen, R. Zheng, J. Wang, H. Wang, M. Li, Y. Wang, H. Lu, Z. Zhang, Y. Liu and Z. Tang, *Journal of Materials Chemistry C*, 9(2021)6937.
28. L. Liu, K. Cao, S. Chen and W. Huang, *Advanced Optical Materials*, 8(2020)2001122.
29. W. Chen, R. Liu, Q. Zeng and L. Zhou, *Solar Energy*, 184(2019)508.
30. H. Wang, M. Wang and Y. Tang, *Energy Storage Materials*, 13(2018)1.
31. N. Balaji, D. Lai, V. Shanmugam, P.K. Basu, A. Khanna, S. Duttagupta and A.G. Aberle, *Solar Energy*, 214(2021)101.
32. A. Yu, Q. Pan, M. Zhang, D. Xie and Y. Tang, *Advanced Functional Materials*, 30(2020)2001440.
33. T. Dullweber, C. Kranz, R. Peibst, U. Baumann, H. Hannebauer, A. Fülle, S. Steckemetz, T. Weber, M. Kutzer and M. Müller, *Progress in Photovoltaics: Research and Applications*, 24(2016)1487.

34. Y.-J. Lee, B.-S. Kim, S. Ifitiquar, C. Park and J. Yi, *Journal of the Korean Physical Society*, 65(2014)355.
35. M. Wang and Y. Tang, *Advanced Energy Materials*, 8(2018)1703320.
36. C. Jiang, L. Xiang, S. Miao, L. Shi, D. Xie, J. Yan, Z. Zheng, X. Zhang and Y. Tang, *Advanced Materials*, 32(2020)1908470.